Phytopathology Research

METHODOLOGY

Open Access

Efficient gene editing with an Arg-tRNA promoter-driven CRISPR/Cas9 in the rice blast fungus *Pyricularia oryzae*

Rui-Jin Wang[1,2†], Jianhui Zhao[1,2†], Vijai Bhadauria[1] and You-Liang Peng[1*]

Abstract

CRISPR/Cas9 technology has been widely adopted for genome editing in a wide range of organisms, including many fungi. *Pyricularia oryzae* is a filamentous fungal pathogen that causes the devastating rice blast disease. However, an efficient and cost-effective CRISPR/Cas9 system for the rice blast fungus has yet to be established. Here, we report an 84-bp arginyl (Arg)-tRNA promoter-driven CRISPR/Cas9 system, which enables efficient and cost-effective gene editing in *P. oryzae*. Preliminary screening of three tRNAs from the 179 predicted tRNAs in *P. oryzae* showed that two Arg-tRNA CRISPR/Cas9 cassettes reproducibly generated MoB56 disruption efficiently. Further, five genes located on distinct chromosomes, including two previously uncharacterized genes, were randomly picked up to test the efficiency of the Mo_tRNA^{Arg24}-gRNA-Cas9 cassette. *Ppg1* is a gene essential to the pathogenicity and important for mycelial growth and conidiation of *P. oryzae*, which is located at chromosome 2 and exhibited a relatively low gene replacement rate (< 1/500) by the traditional gene replacement approach. By using the Mo_tRNA^{Arg24}-gRNA-Cas9 cassette, *Ppg1* gene disruption rate was increased up to 75.9%. In addition, *Bip2*, an uncharacterized genes located close to the centromere of chromosome 4, was disrupted at 66.7%. For all the five tested genes, our Mo_tRNA^{Arg24}-gRNA-Cas9 cassette showed high gene disruption efficiency in *P. oryzae*, ranging from 66.7% to 100%. Importantly, it rarely induces Cas9 toxicity to *P. oryzae*. The Mo_tRNA^{Arg24}-gRNA-Cas9 cassette described in this study can be adopted as an alternative for functional genomics study in *P. oryzae*.

Keywords Rice blast fungus, Arg-tRNA promoter, CRISPR/Cas9, Gene disruption

Background

The filamentous fungus *Pyricularia oryzae* (syn. *Magnaporthe oryzae*) causes blast diseases in a number of agronomically important crops, including rice, wheat, and finger millet (Wilson and Talbot 2009). *P. oryzae* has been adopted as a seminal model to investigate host-fungal pathogen interactions. Homology recombination (HR)-based gene replacement with selectable markers has been widely used for decades to disrupt genes in *P. oryzae*, but this approach depends on low native HR rate, requiring heavy works to obtain gene disrupted mutants. Clustered regularly interspaced short palindromic repeats (CRISPR)/Cas9 systems significantly improve the HR frequency and has been adopted for gene disruption in several fungal pathogens (Song et al. 2019; Zhang et al. 2019). However, an efficient and cost-effective CRISPR/Cas9 system for *P. oryzae* has not been established.

†Rui-Jin Wang and Jianhui Zhao contribute equally to this work.

*Correspondence:
You-Liang Peng
pengyl@cau.edu.cn
[1] MOA Key Laboratory for Monitoring and Green Management of Crop Pests, College of Plant Protection, China Agricultural University, Beijing 100193, China
[2] MARA Key Laboratory of Pest Monitoring and Green Management, College of Plant Protection, China Agricultural University, Beijing 100193, China

A CRISPR/Cas9 system contains two essential components: a functional Cas9 endonuclease and a small guide RNA (gRNA) that directs Cas9 to a specific DNA sequence (Cong et al. 2013). Cas9 cleaves the target DNA strand, leading to double-strand break (DSB) repair, which triggers targeted gene editing via canonical non-homologous end joining (C-NHEJ) or via homology repair if a DNA homologous template (donor DNA) is provided (Her and Bunting 2018). The targeting capability of the CRISPR/Cas9 system is largely constrained by the gRNA-expressing and processing efficiency. Several types of promoters have been applied for highly expressing gRNAs, including RNA polymerase type II promoters (pol II), RNA polymerase type III promoters (pol III), and in vitro transcribed T7 promoters. The pol III promoters are the most widely used, including U6 snRNA promoters, 5S rRNA promoters, tRNA promoters, and SNR52 promoters (Song et al. 2019). In most cases, gRNA is driven by U6 promoters. However, the U6 promoter transcribes gRNA with some limitations, which limit the CRISPR target sequences to G(N)20GG (Gao and Zhao 2014). And low sequence conservation of the U6 snRNA gene also made it challenging to identify the U6 promoter in some fungi, such as *Ustilaginoidea virens* (Liang et al. 2018). In addition to the U6 promoter, tRNA promoters are widely used for gRNA expression due to its significant advantages. tRNA promoters display high driving efficiencies of gRNA expression in many fungi (Liang et al. 2018), and their cleavable capability makes them suitable for multiplexed genome editing (Xie et al. 2015; Zhang et al. 2019). In addition, tRNAs are not constrained by certain sequence specificity. The 5S rRNA promoter has also been used to drive gRNA in *Trichoderma atroviride*, which shows higher gene disruption efficiency than the U6 promoter (Zheng et al. 2019). In *Saccharomyces cerevisiae*, the SNR52 promoter was used to drive gRNA expression. Its combination with the tRNA promoter displays high efficiency for multiplexed genome editing (Zhang et al. 2019). Thus, selecting a promoter for driving gRNA expression represents an important technical step in the development of an efficient CRISPR/Cas9 genome editing system.

In *P. oryzae*, several CRISPR/Cas systems have been tested. The CRISPR/Cas9 system with U6 promoters successfully knocked out the *SDH* gene with an efficiency of 36.1–83.6% via different gRNA sites, which is higher than the CRISPR/Cas9 system with TrpC promoter (Arazoe et al. 2015). However, Foster et al. reported that the CRISPR/Cas9 system with U6 promoter did not work well in their knockout experiments whereas they used an in vitro-assembled CRISPR/Cas9 system to disrupt *ALB1* and *RSY1* with high efficiency (Foster et al. 2018). Recently, the CRISPR/Cas12a ribonucleoprotein genome editing system has also been tested in *P. oryzae* (Huang et al. 2022). Since U6 promoter-driven gRNA expression is not always stable, and commercial Cas9 proteins needs additional expense, a more efficient and cost-effective CRISPR/Cas9 system is required for *P. oryzae*.

Various tRNA promoters have been tested in fungi, and the genome editing efficiency of different tRNA promoters varies greatly in a strain-dependent manner (Song et al. 2019). In *Ustilago maydis*, four tRNA promoters, $tRNA^{LeuTAA}$, $tRNA^{GlyGCC}$, $tRNA^{TyrGTA}$, and $tRNA^{GlyTCC}$ were tested, all of which showed higher efficiencies of gRNA expression than the U6 promoter (Schuster et al. 2018). In *U. virens*, a 72 bp $tRNA^{GlnTTG}$ promoter significantly increased HR rate (Liang et al. 2018). In *Aspergillus niger*, 37 tRNAs for 18 amino acids were tested, and 36 of the 37 tRNAs were able to generate mutation with similarly high efficiencies, except for a 92 bp $tRNA^{GlnTTG}$ (Song et al. 2018). In *Colletotrichum higginsianum*, a gln-tRNA-based CRISPR/Cas9 knockout system showed 100% gene replacement frequency (Bhadauria et al. 2024). In *S. cerevisiae*, tandem $tRNA^{Gly}$ promoters were used for multiplexed genome editing, enabling simultaneous disruption of 8 genes with 87% efficiency (Zhang et al. 2019). In *Yarrowia lipolytica*, a $tRNA^{Gly}$-driven CRISPR/Cas9 system disrupted *PEX10* at only 30% (Schwartz et al. 2016). It remains unclear which tRNA promoter can drive efficiently gRNA expression in the rice blast fungus *P. oryzae*.

In this study, we developed a highly efficient gene disruption protocol for *P. oryzae* by using an Arg-tRNA promoter-driven CRISPR/Cas9 system. To evaluate gene disruption efficiency by the protocol, we randomly picked up five genes that were located in different chromosomes. Our results show that the gene disruption frequency ranged from 66.7% to 100.0%. In addition, our CRISPR/Cas9 system rarely induces Cas9 toxicity to *P. oryzae*. Thus, our Arg-tRNA promoter-driven CRISPR/Cas9 system may be adopted as an alternative for functional genomics study in *P. oryzae*.

Results

Selection of tRNA genes for constructing gRNA transcription cassettes

To screen tRNA genes for constructing gRNA transcription cassettes, we first analyzed the whole genome of *P. oryzae* strain P131 with the tRNAscan-SE program 2.0 (Chan and Lowe 2019), and predicted a total of 179 non-redundant tRNA genes (Additional file 1: Table S1). We then used the pCas9-tRp-gRNA vector for *U. virens* genome editing (Liang et al. 2018) as a framework to construct the tRNA-driven gRNA transcription cassettes for testing which tRNA promoter is highly efficient for *P. oryzae* gene disruption. Three tRNA gene promoters were

chosen for the test, including two $tRNA^{Arg}$ promoters. A previous study reported that two $tRNA^{Arg}$ (anticodon ACG) promoters display high efficiency in driving gRNA transcription in *A. niger* (Song et al. 2018). In *P. oryzae*, there are 14 tRNA genes that recognize Arg anticodon, seven of which recognize ACG anticodon. Considering that a relatively short tRNA may impart simple and compact architecture to sgRNA cassette and enable efficient transcription (Zhang et al., 2019), we chose two shortest $tRNA^{Arg(ACG)}$ genes, named $tRNA^{Arg17}$ and $tRNA^{Arg24}$, respectively, to drive gRNA expression (Fig. 1a and Additional file 1: Table S1). In addition, we also tested the 96-bp $tRNA^{Gln14}$ (Additional file 1: Tbale S1). All the cassettes contain four elements: the tRNA gene of *P. oryzae*, gRNA spacer insertion region for inserting target sequence via *Bsm*BI sites, gRNA scaffold and terminator, and together with tef (the translation elongation factor) promoter-driven Cas9 cassette that were named as Mo_tRNA-gRNA-Cas9 vectors.

To acheive gene disruption, a DNA fragment for corresponding sgRNA of each target gene was inserted into *Bsm*BI sites to generate Mo_tRNA-sgRNA (specific gene)-Cas9 vector, which was then co-transformed into the protoplasts of *P. oryzae* with the gene replacement vector pKOV21 that carries hygromycin B phosphotransferase gene (*Hyg*) as a positive selection marker and neomycin/G418 resistance gene (*Neo*) as a negative selection marker (Fig. 1b).

To determine which of the three tRNA genes is reproducibly efficient for gene disruption in *P. oryzae*, we first tried to disrupt *MoB56* in the *P. oryzae* strain P131. *MoB56*, encoding a regulatory subunit of PP2A, is located on the chromosome 6 (Fig. 2a), and showed relatively low disruption rate with the classical gene replacement method (Wang et al. 2023). Our preliminary test results showed that, in co-transformation with the pKOV21 vector, both Mo_$tRNA^{Arg17}$-gRNA-Cas9 and Mo_$tRNA^{Arg24}$-gRNA-Cas9 cassettes

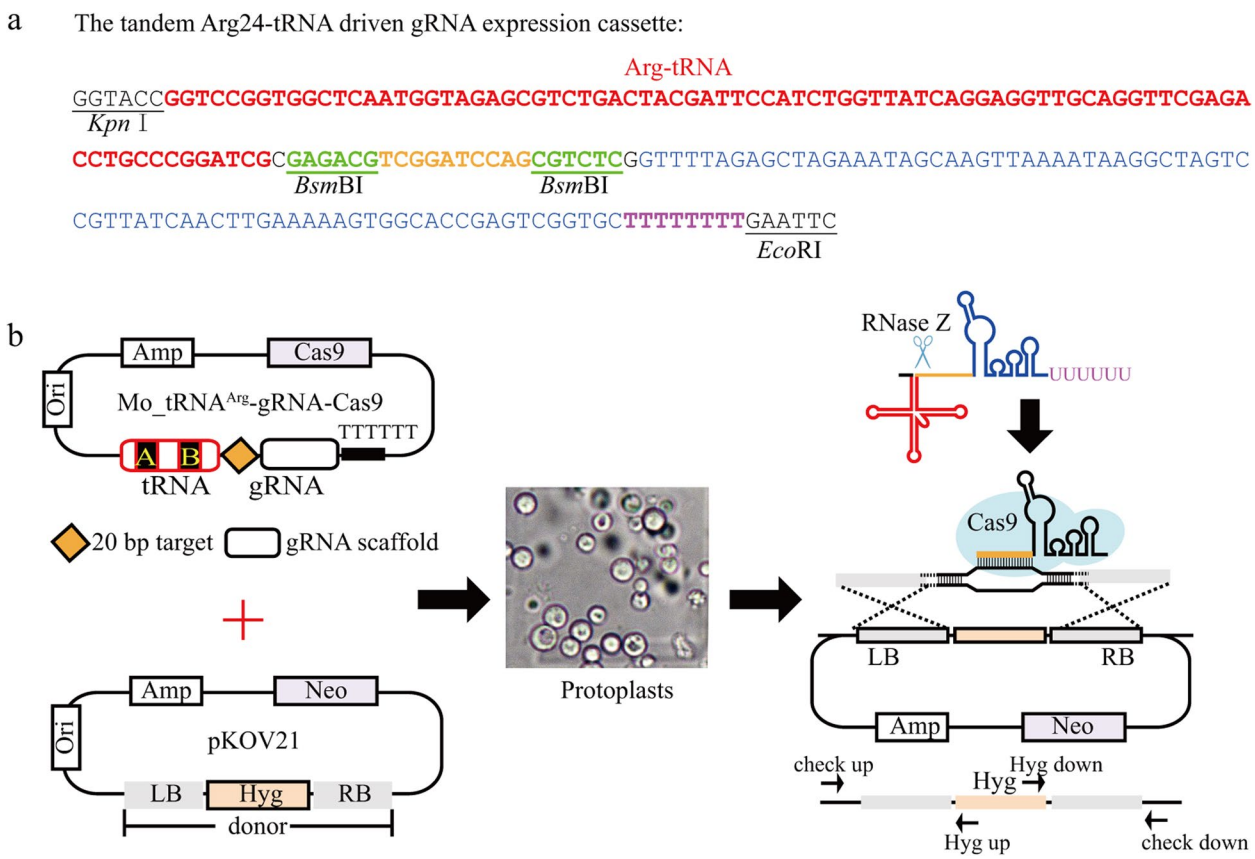

Fig. 1 The shematic diagram of the Arg-tRNA driven gRNA-Cas9/kov21 gene replacement system in *P. oryzae*. **a** The tandem Arg-tRNA driven gRNA expression cassette, which includes an 84 bp $tRNA^{Arg(ACG)}$ gene of *P. oryzae* (red), gRNA spacer insertion region for inserting target sequence via *Bsm*BI sites (green and underlined), gRNA scaffold (blue), and terminator (purple). **b** The strategy of the Arg-tRNA driven CRISPR/Cas9 system for efficient gene disruption in *P. oryzae*. The constructed Mo_$tRNA^{Arg}$-gRNA-Cas9 vector with 20-bp target sgRNA co-transformed with donor pKOV21 vector into protoplast to generate sgRNA and induce gene replacement. Two pairs of primers, Check up/Hyg up and Check down/Hyg down are used to confirm correct gene knock-out mutants

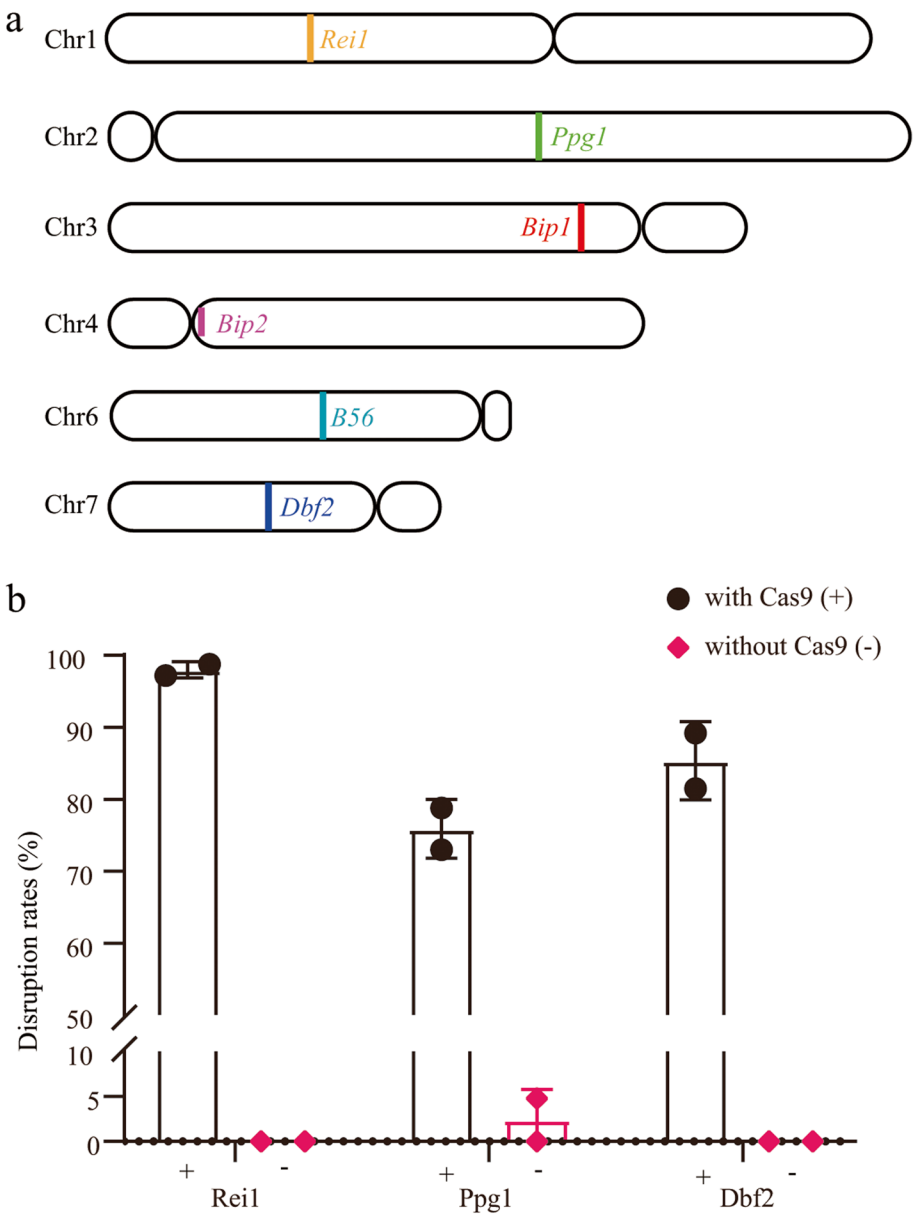

Fig. 2 Efficient gene disruptions with the Mo_tRNA^{Arg}-gRNA-Cas9/pKOV21 system in *P. oryzae*. **a** The loci of selected genes for assessing the efficiency of the Mo_tRNA^{Arg}-gRNA-Cas9/pKOV21 system in *P. oryzae*. Six selected genes are located in different chromosomes, and *Bip2* is quite close to the centromere on chromosome 4. Scale bars = 1 Mbp. **b** The gene replacement rates of three reported genes with the Mo_tRNA^{Arg}-gRNA-Cas9/pKOV21 system

reproducibly generated *MoB56* disruption mutants at rates from 63 to 83%, which are much higher than the rates generated by Mo_tRNA^{Gln14}-gRNA-Cas9 (Additional file 2: Table S2). Subsequently, we used Mo_tRNA^{Arg24}-gRNA-Cas9 as a gRNA transcription cassette for checking disruption efiiciency of other genes in *P. oryzae*.

An Arg-tRNA promoter-driven CRISPR/Cas9 system significantly increased gene replacement rate in *P. oryzae*

We ramdomly selected three previously reported genes (Fig. 2a), *Rei1*, *Ppg1*, and *Dbf2* that locate on chromosomes 1, 2, and 7, respectively, to further test the efficiency of Mo_tRNA^{Arg24}-gRNA-Cas9 in *P. oryzae*. Disruption of *Rei1*, *Ppg1*, and *Dbf2* in *P. oryzae*

had significant defects on mycelial growth (Du et al. 2013; Cao et al. 2016; Feng et al. 2021). The sgRNA target sequences of the three genes were analyzed by sgRNA designer programs (Additional file 3: Table S3), and were independently inserted into the gRNA spacer insertion region of Mo_tRNA^{Arg24}-gRNA-Cas9 vector, co-transformation of Mo_tRNA^{Arg24}-gRNA-Cas9 with the traditional gene replacement vector pKOV21 reproducibly generated *Rei1*, *Ppg1*, and *Dbf2* mutants at rates 98.0%, 75.9%, and 85.4%, respecitively (Fig. 2b and Additional file 4:Table S4). We selected the Hyg-resistant and Neo-sensitive transformants and cultured them on oatmeal tomato agar (OTA) plates to observe their phenotypes. The results showed that most of the transformants displayed knock-out mutant phenotype (Fig. 3d–f). We then randomly selected 10 transformants of each gene with knock-out mutant phenotype for PCR verification with Hyg-up/Check-up and Hyg-down/Check-down primers as shown in the schematic diagram (Fig. 3a–c). The results showed that all the 10 selected transformants for each gene were correct gene disruption mutants (Fig. 3g–i). Three mutants of each gene were then randomly picked up to test their phenotypes on growth, which displayed the same growth defects as presiously reported (Fig. 3m–o).

Expression of Cas9 was transient and not toxic to *P. oryzae*

Foster et al. reported that the constitutive expression of *Cas9* is toxic to *P. oryzae*, resulting in less number of tranformants generated (Foster et al. 2018). We thus further evaluated whether our strategy for genome editing results in toxicity of Cas9 to *P. oryzae*. We found that the number of transformants generated from the co-transformation of Mo_tRNA^{Arg24}-gRNA-Cas9 vectors with pKOV21 vectors was even much more than those generated from the transformation with only pKOV21 vectors (Additional file 5: Table S5), indicating the Mo_tRNA-gRNA-Cas9 system is not toxic to *P. oryzae*. Furthermore, we tested whether the *Cas9* gene was integrated into the genome of *P. oryzae*. PCR amplification of partial *Cas9* sequence showed that none of the replacement mutants of *Rei1* contained *Cas9* (Fig. 3j), and only one and two transformants carrying *Cas9* were amplified from the randomly selected 10 mutants of *Ppg1* and *Dbf2*, respectively (Fig. 3k, l). These results indicate *Cas9* is transiently expressed in most cases and rarely integrated into the genome if co-transformation of Mo_tRNA^{Arg24}-gRNA-Cas9 vector with pKOV21 vector for disrupting a gene in *P. oryzae*.

Identifcation of two genes important for conidiation in *P. oryzae* through the Mo_tRNA^{Arg24}-gRNA-Cas9 mediated gene disruption

To further verify the high efficiency of the Mo_tRNA^{Arg24}-gRNA-Cas9 system for disrupting genes in *P. oryzae*, we randomly picked up two hypothetical genes (MGG_05198 and MGG_03741) for disruption, which were located on chromosome 3 and 4 and named as *Bip1* and *Bip2* (Fig. 2a), respectively. For *Bip1* gene disruption (Fig. 4a), a total of 89 G418-sensitive transformants were generated. We randomly picked up ten of them for PCR verification (Fig. 4b), all of which were confirmed to be correct disruption mutants without *Cas9* in their genomes (Fig. 4c), including three mutants that were further confirmed by Southern blot (Fig. 4d). For disrupting *Bip2* (Fig. 4e), which is quite close to the centromere of chromosome 4 (Fig. 2a), a total of six G418-sensitive transformants were obtained, four of which were correct disruption mutants verified by PCR (Fig. 4f), including three were further confirmed by Southern blot (Fig. 4g). None of these *Bip2* disruption mutants contain *Cas9* in their genomes (Fig. 4h).

To identify the role of *Bip1* and *Bip2* in *P. oryzae*, we assayed phenotypes of *Δbip1* and *Δbip2*. The *Δbip1* and *Δbip2* mutants were similar to the wild-type strain in colony growth after 5 days of culturing on OTA plates (Fig. 5a, b, d, and e), indicating that they are not important for mycelial growth. However, as compared with their wild-type strain, *Δbip1* and *Δbip2* mutants were decreased in conidiation by ~ 50% (Fig. 5c) and by ~ 30% (Fig. 5f), respectively, indicating that *Bip1* and *Bip2* are important for conidiation.

Discussion

Recently developed CRISPR/Cas9 system has greatly accelerated the speed of genome editing in a wide range of organisms. In *P. oryzae*, U6 and TrpC promoters were used to drive gRNA expression for gene editing, showing efficient disruption of *SDH* and *SRS2* (Arazoe et al. 2015). Whereas, Foster et al. reported that the U6 promoter sometimes worked not well, and in replace, they used purified Cas9 protein along with in vitro synthesized sgRNA complex to increase gene disruption efficiency in *P. oryzae* (Foster et al. 2018), which led to efficient disruption of *ALB1* and *RSY* in *P. oryzae* but required additional cost to buy purified Cas9. Here, we reported that an 84-bp Arg-tRNA gene is efficient for driving gRNA transcription and that its derived Mo_tRNA^{Arg24}-gRNA-Cas9 in combination with the traditional gene replacement vector pKOV21 can be used to achieve highly efficient gene disruption in *P. oryzae*. We evaluated its efficiency by disrupting six genes, including a gene

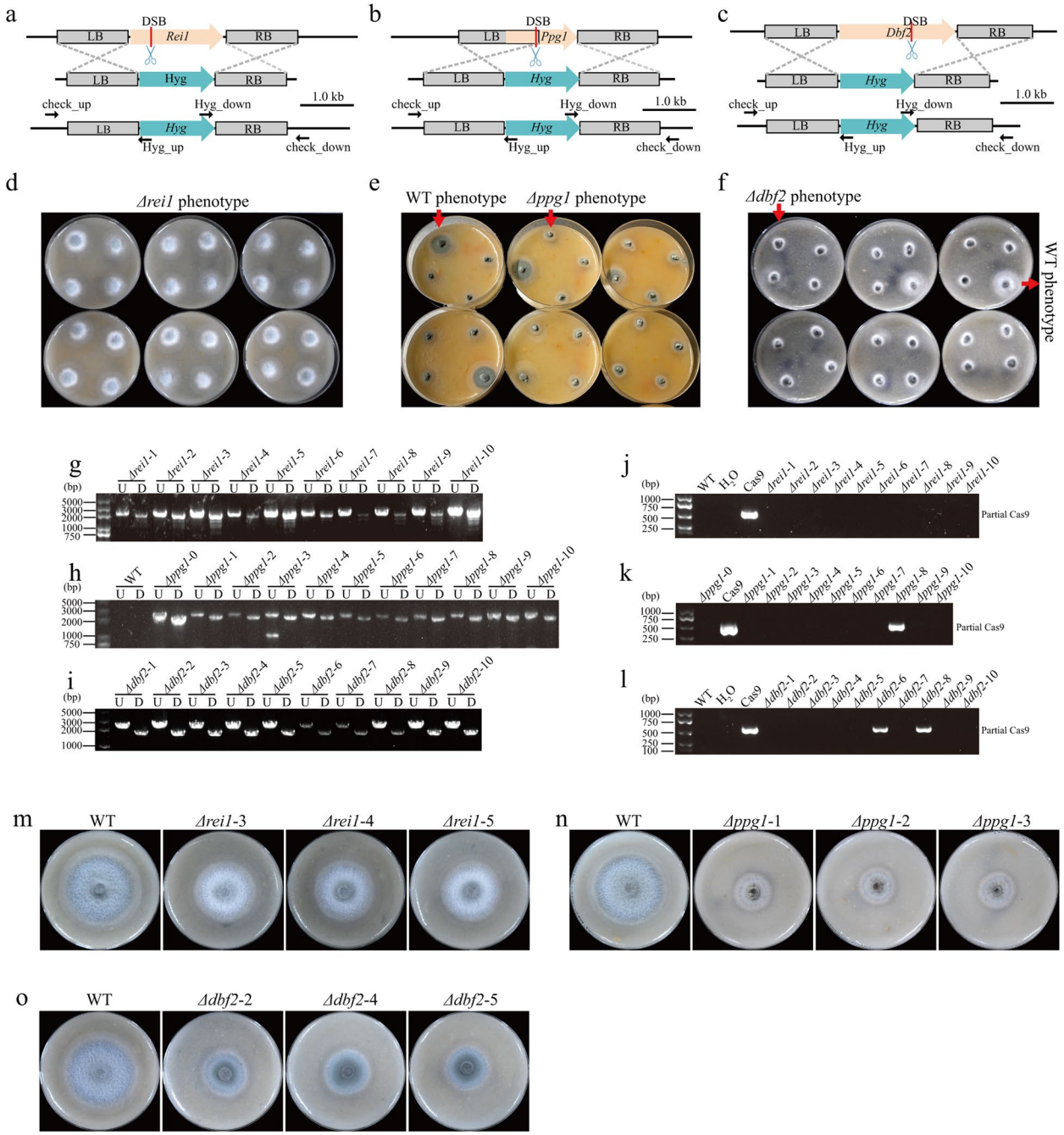

Fig. 3 Gene disruption of three reported genes, *Rei1*, *Ppg1*, and *Dbf2*, via Mo_tRNA^{Arg}-gRNA-Cas9/pKOV21 system. **a**–**c** Strategy of gene replacement for genes, the sgRNA-guided Cas9-induced double-strand break (DSB) sites was indicated with scissor symbol. **d**–**f** Phenotype of 24 randomly selected G418-sensitive transformants of each gene disruption. **g**–**i** PCR verification using the Hyg_up/check_up and Hyg_down/check_down primers (as indicated in **a**–**c**) to confirm the correct replacement of each gene with *Hyg*. Ten random transformants with the correct knockout mutant phenotype of each gene were selected. In Fig. 3 h, the wild-type P131 and *Δmoppg1*-0 were used as negative and positive controls, respectively. **j**–**l** PCR detection for *Cas9* insertion into genomes of the ten transformants of each gene mentioned in **g**–**i**. In Fig. 3g, i, the genomic DNA of the wild-type strain P131 and water were used as negative controls. The Mo_tRNA-gRNA-Cas9 vector was used as positive control. In Fig. 3k, *Δmoppg1*-0 was used as a negative control. **m**–**o** Colony phenotypes of each gene disruption strains and wild-type strain P131 cultured on OTA plates for 5 days

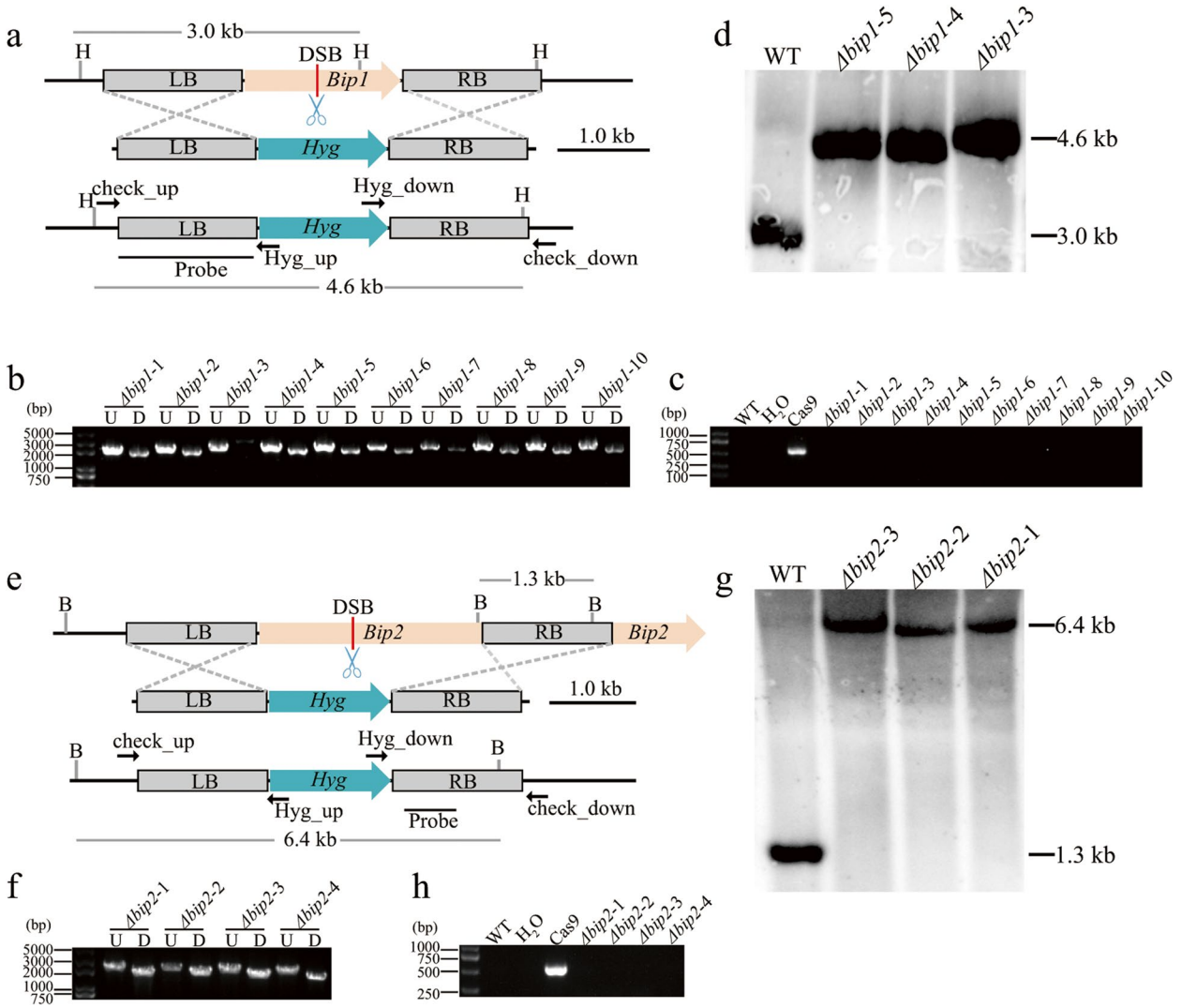

Fig. 4 Disruptions of two uncharacterized genes, *Bip1* and *Bip2*, with Mo_tRNA^{Arg}-gRNA-Cas9/pKOV21 system in *P. oryzae*. **a** Strategy for *Bip1* gene replacement, including the sgRNA-guided Cas9-induced DSB site on *Bip1*. H indicates *Hind* III used to digest genomic DNAs for Southern blot. The probe used for Southern blot was labeled. **b** Ten Neo-sensitive transformants were checked by PCR with the Hyg_up/check_up and Hyg_down/check_down primers (as shown in **a**) to verify *Bip1* replaced by *Hyg* correctly. **c** PCR detection of *Cas9* insertion in genomes of the ten transformants mentioned in **b**. **d** *Δbip1* mutants verified by Southern blot. **e** Strategy for *Bip2* gene replacement, B indicates *Bgl* II used to digest genomic DNAs for Southern blot. The probe used for Southern blot was labeled. **f** Four Neo-sensitive transformants were checked by PCR to verify correct replacement of *Bip2* by *Hyg*. **g** Southern blot for verifying *Δbip2* mutants. **h** PCR detection for *Cas9* insertion in genomes of the transformants in **f**

located near the centromere of chromosome 4 (Fig. 2). Our results showed that the system could reproducibly result in gene disruption in *P. oryzae* at a high frequency, ranging from 66.7%–100.0% (Figs. 2b, 4, and Additional file 4: Table S4). Thus, our system, the Mo_tRNA^{Arg24}-gRNA-Cas9/pKOV21 cotransformation, can be adopted as an alternative for highly efficient gene disruption in *P. oryzae*.

In *A. niger*, 36 tRNAs for 18 amino acids showed similar high efficiency, including two Arg-tRNAs (anticodon ACG), whereas a 92-bp Gln-tRNA (anticodon TTG) showed low efficiency for gene disruption (Song et al. 2018). In *U. virens* and *C. higginsianum*, Gln-tRNA (anticodon TTG) showed high gene disruption efficiency (Liang et al. 2018; Bhadauria et al. 2024). In the present study, we showed that the gene disruption efficiency by a 95-bp Gln-tRNA derived vector (anticodon CTG) was < 50% while two 84-bp Arg-tRNA (Arg17 and Arg24) derived vectors (anticodon ACG) are similarly high-efficient (Additional file 2: Table S2). Thus, different tRNAs may vary in their efficiency in driving gRNA expression. Besides tRNA^{Arg24}, other tRNAs may

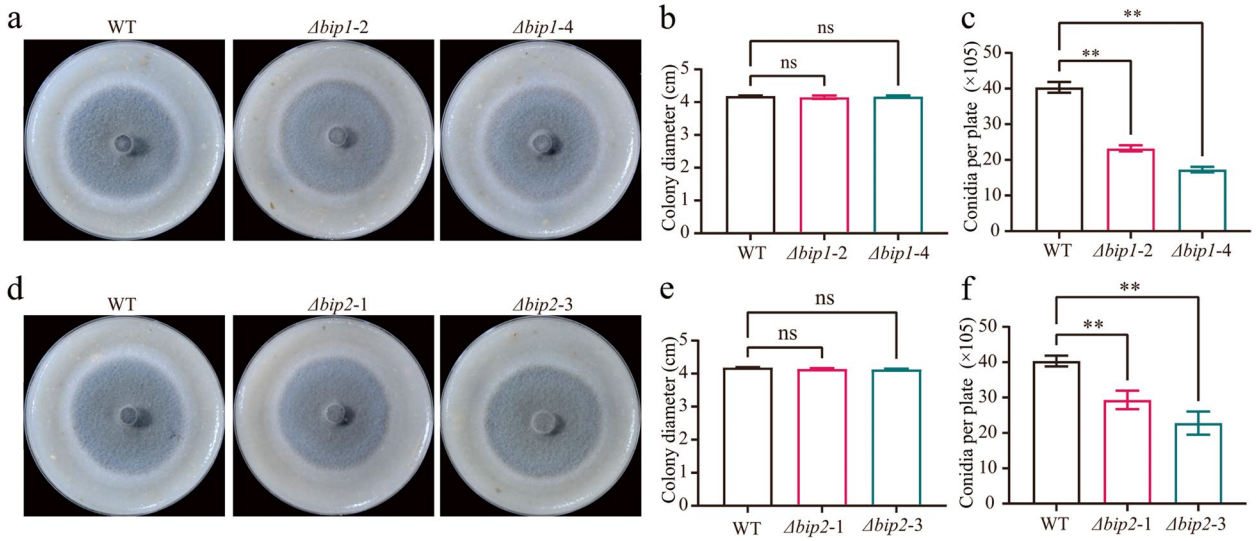

Fig. 5 *Bip1* and *Bip2* are important for conidiation. **a** Colonies of the wild-type strain and two *Δbip1* mutants cultured on OTA plate for 5 days. **b** The colony diameters of the strains as mentioned in **a**. **c** Conidiation of the strains mentioned in **a**. **d** Colony comparison of wild-type strain and two *Δbip2* mutants cultured on OTA plate for 5 days. **e** The colony diameters of the strains as mentioned in **d**. **f** Conidiation of the strains mentioned in **d**. ** $p < 0.01$; ns, not statistically significant

also be efficient to drive gRNA expression in *P. oryzae*, such as $tRNA^{Arg17}$. In addition, a U6 promoter can drive gRNA expression for highly efficient disruption of *SDH* and *SRS2* in the strain Hoku-1 but seemed not to work well in the Guy11 strain of *P. oryzae* (Arazoe et al. 2015; Foster et al. 2018). Thus, the same vector may differ in their efficiency in different strains. Although we verified that our Mo_$tRNA^{Arg24}$-gRNA-Cas9/pKOV21 is highly efficient for gene disruption in the P131 strain, it remains to be checked whether this system works well in other strains of *P. oryzae*.

Foster et al. reported that the constitutive expression of *Cas9* is toxic to *P. oryzae*, resulting less generation of transformants (Foster et al. 2018). This showed that equal or even more transformants can be obtained by co-transforming Mo_$tRNA^{Arg24}$-gRNA-Cas9/pKOV21 vectors, not less than those obtained by transformation with the pKOV21 vector that does not carry *Cas9* (Additional file 2: Table S2 and Additional file 4: Table S4). In fact, *Cas9* was detected in very few transformants generated by cotransforming Mo_$tRNA^{Arg24}$-gRNA-Cas9/pKOV21 vectors (Figs. 3j, i and 4c, h), suggesting that *Cas9* is transiently expressed in the system. In addition, this system generates mutants by homologous recombination enhanced by DSB generated by Cas9 transiently expressed from the Mo_$tRNA^{Arg24}$-gRNA-Cas9, which undergos two rounds of selection, a positive selection based on hygromycin B phosphotransferase (Hyg resistance gene) gene and a negative selection based on neomycin/G418 resistance gene on the pKOV21 vector (Yang et al. 2010), thus increasing frequency of gene disruption.

In *Aspergillus*, AMA1-based plasmid is generally used to construct a genome-editing system, allowing for autonomous plasmid replication and increasing mutation efficiencies (Song et al. 2019; Li et al. 2021). This stratergy may be considered for application in *P. oryzae* to further improve tRNA-gRNA-CRISPR/Cas9 efficiency.

Conclusion

The present study reported that an 84-bp Arg-tRNA promoter is highly efficient in driving gRNA transcription in the rice blast fungus *P. orzyae*, and its cassette with Cas9 can highly improve gene replacement efficiency of pKOV21 by homologous recombination in the fungus. Thus, our Arg-tRNA promoter-driven CRISPR/Cas9/pKOV21 system provides an alternative for functional genomics study in *P. oryzae*.

Methods

Strains and cultural conditions

Storage, maintenance, and growth of the *P. oryzae* strains, and nucleic acid extraction were carried out as described previously (Wang et al. 2023).

The tRNA gene prediction and selection

The tRNA genes for this study were retrieved from the genome of the *P. oryzae* P131 strain. All potential tRNA genes in *P. oryzae* were predicted by the online program tRNAscan-SE version 2.0 (Chan and Lowe 2019).

Sequences of the selected Arg tRNA gene in this study were listed in Additional file 1: Table S1.

Construction of the Mo_tRNA^{Arg}-gRNA-pCas9 vector

The tRNA^{Arg24}-gRNA cassette containing two *Bsa*I sites was assembled by fusion PCR of two fragments. The first fragment containing the tRNA^{Arg24} promoter, gRNA spacer sequence, and gRNA scaffold was generated by primers F1 and R1. The tRNA^{Arg} promoter with 20 bp gRNA spacer sequence containing *Bsa*I sites was synthesized into primer gRNA-F1. The 20 bp gRNA spacer sequence was used as an overlapping sequence. The second fragment containing gRNA spacer, gRNA scaffold and terminator was generated by primers F2 and R2. Primers gRNA-F1 and gRNA-R2 were used to assemble the two fragments together, and primers F0/R0 were used to clone the assembled cassette to the *Hind*III and *Eco*RI sites of vector pUC19 plasmid. A short cassette with two *Bsm*BI sites was generated by annealing the sense (LINK-SEQ-L) and the antisense (LINK-SEQ-R) oligonucleotides and inserted between the two *Bsa*I sites of the pUC19-tRNA-gRNA vector by Golden Gate cloning (New England Biolabs, Ipswich, MA, United States) to generate the pUC19-LINK vector. The tRNA^{Arg24} -gRNA cassette with two *Bsm*BI sites was amplified with C9TSG-F and C9TSG-R and cloned between the *Kpn*I and *EcoR*I sites of the *U. virens* pCas9-tRp-gRNA vector (Liang et al. 2018) to generate the Mo_tRNA^{Arg24}-gRNA-Cas9 vector. Similar statergies were used for construction of other Mo_tRNA-gRNA-Cas9 vectors. All primers used for vector construction were listed in Additional file 5: Table S5.

Identification of guide sequences and construction of specific tRNA-sgRNA-Cas9 vectors for each gene

The 20-bp guide RNA sequences of *MoB56*, *Dbf2*, and *Ppg1* were designed with the gRNA designer program CRISPick (https://portals.broadinstitute.org/gppx/crispick/public). The guide RNA sequences of *Rei1*, *Bip1*, and *Bip2* were designed using E-CRISP (http://www.e-crisp.org/E-CRISP/). The guide sequences were inserted into the two *Bsm*BI sites within the gRNA spacer of the Mo_tRNA^{Arg}-gRNA-Cas9 vector. Additional file 3: Table S3 shows the guide sequences used in this study.

Construction of the gene replacement vectors

Targeted genes were replaced with the hygromycin B phosphotransferase (*Hyg*) gene. For the construction of gene replacement vectors, the ~ 1.5 kb upstream and ~ 1.5 kb downstream fragments of each gene were amplified and cloned into pKOV21. The primers used were listed in Additional file 5: Table S5.

Transformation, mutant purification, and screening

Transformation and genomic DNA isolation of *P. oryzae* strains were performed as previously described (Wang et al. 2023). All transformations were carried out using 1–1.5 μg of the donor pKOV21-based replacement plasmid per tube with or without tRNA-gRNA-Cas9 vector when needed. The amount ratio of donor pKOV21 to tRNA-gRNA-Cas9 was 1:1. Mutant clones were visually identified according to colony morphology first and double-checked with PCR. The CRISPR efficiency was calculated by dividing the number of mutant colonies by the total number of transformants after negative selection for Neo-resistance. Cases where Cas9 was inserted and integrated into the *P. oryzae* genome was detected by PCR. All primers used were listed in Additional file 5: Table S5.

Southern blot assay for *Bip1* and *Bip2* replacement mutants

Genomic DNA of *Δbip1* and *Δbip2* mutants were digested by *Hind* III and *Bgl* II, respectively. The upstream fragment of *Bip1* was used as a probe to detect and distinguish the wild-type strain and *Δbip1* mutants. The downstream fragment of *Bip2* was used as a probe to detect and distinguish the wild-type strain and *Δbip2* mutants. The schematic diagrams of Southern blot strategies are shown in Fig. 4a, e.

Mycelial growth and conidiation assays

Colony blocks of all strains were cultured on OTA plates, and colony diameters of each strain were measured after 5 d of culture. Conidiation was calculated after 6 d of culture. Three replicates were conducted.

Abbreviations

CRISPR	Clustered regularly interspaced short palindromic repeats
DSB	Double-strand break
HR	Homology recombination

Supplementary Information

The online version contains supplementary material available at https://doi.org/10.1186/s42483-024-00271-8.

Additional file 1: Table S1. The 179 non-redundant tRNA genes predicted in P131 genome.

Additional file 2: Table S2. Gene disruption rates of MoB56 with different Mo_tRNA-gRNA-Cas9/pKOV21 systems.

Additional file 3: Table S3. sgRNAs designed for gene disruption in this study.

Additional file 4: Table S4. The gene replacement rates of three reported genes with the Mo_tRNA^{Arg}-gRNA-Cas9/pKOV21 system.

Additional file 5: Table S5. Primers used in the study.

Acknowledgements
We thank Professor Jin-Rong Xu at Purdue University for providing the *U. virens* pCas9-tRp-gRNA vector as gift.

Authors' contributions
RW and YP designed experiments; RW and ZJ performed the experiments and analyzed the data; RW draft the manuscript, RW, YP, and VB revised the manuscript. All authors read and approved the final manuscript.

Funding
This work was supported by the National Natural Science Foundation of China (32000104), and Agriculture Research System of China (CARS-01–43) for the design of the study and collection, analysis, and interpretation of data.

Availability of data and materials
Not applicable.

Declarations

Ethics approval and consent to participate
Not applicable.

Consent for publication
Not applicable.

Competing interests
The authors declare that they have no competing interests.

Received: 12 April 2024 Accepted: 2 July 2024
Published online: 10 October 2024

References

Arazoe T, Miyoshi K, Yamato T, Ogawa T, Ohsato S, Arie T, et al. Tailor-made CRISPR/Cas system for highly efficient targeted gene replacement in the rice blast fungus. Biotechnol Bioeng. 2015;112:2543–9. https://doi.org/10.1002/bit.25662.

Bhadauria V, Han TL, Li GJ, Ma WD, Zhang MY, Yang J, et al. A gln-tRNA-based CRISPR/Cas9 knockout system enables the functional characterization of genes in the genetically recalcitrant brassica anthracnose fungus *Colletotrichum higginsianum*. Int J Biol Macromol. 2024;254. https://doi.org/10.1016/j.ijbiomac.2023.127953.

Cao HJ, Huang PY, Zhang LL, Shi YK, Sun DD, Yan YX, et al. Characterization of 47 Cys2-His2 zinc finger proteins required for the development and pathogenicity of the rice blast fungus *Magnaporthe oryzae*. New Phytol. 2016;211:1035–51. https://doi.org/10.1111/nph.13948.

Chan PP, Lowe TM. tRNAscan-SE: Searching for tRNA genes in genomic sequences. Methods Mol Biol. 2019;1962:1–14. https://doi.org/10.1007/978-1-4939-9173-0_1.

Cong L, Ran FA, Cox D, Lin SL, Barretto R, Habib N, et al. Multiplex genome engineering using CRISPR/Cas systems. Science. 2013;339:819–23. https://doi.org/10.1126/science.1231143.

Du Y, Shi Y, Yang J, Chen X, Xue M, Zhou W, et al. A serine/threonine-protein phosphatase PP2A catalytic subunit is essential for asexual development and plant infection in *Magnaporthe oryzae*. Curr Genet. 2013;59:33–41. https://doi.org/10.1007/s00294-012-0385-3.

Feng W, Yin Z, Wu H, Liu P, Liu X, Liu M, et al. Balancing of the mitotic exit network and cell wall integrity signaling governs the development and pathogenicity in *Magnaporthe oryzae*. PLoS Pathog. 2021;17:e1009080. https://doi.org/10.1371/journal.ppat.1009080.

Foster AJ, Martin-Urdiroz M, Yan X, Wright HS, Soanes DM, Talbot NJ. CRISPR-Cas9 ribonucleoprotein-mediated co-editing and counterselection in the rice blast fungus. Sci Rep. 2018;8. https://doi.org/10.1038/s41598-018-32702-w.

Gao YB, Zhao YD. Self-processing of ribozyme-flanked RNAs into guide RNAs in vitro and in vivo for CRISPR-mediated genome editing. J Integr Plant Biol. 2014;56:343–9. https://doi.org/10.1111/jipb.12152.

Her J, Bunting SF. How cells ensure correct repair of DNA double-strand breaks. J Biol Chem. 2018;293:10502–11. https://doi.org/10.1074/jbc.TM118.000371.

Huang J, Rowe D, Subedi P, Zhang W, Suelter T, Valent B, et al. CRISPR-Cas12a induced DNA double-strand breaks are repaired by multiple pathways with different mutation profiles in *Magnaporthe oryzae*. Nat Commun. 2022;13. https://doi.org/10.1038/s41467-022-34736-1.

Li Y, Zhang H, Fan J, Chen Z, Chen T, Zeng B, et al. A highly efficient identification of mutants generated by CRISPR/Cas9 using the non-functional DsRed assisted selection in *Aspergillus oryzae*. World J Microbiol Biotechnol. 2021;37(8):132. https://doi.org/10.1007/s11274-021-03100-8.

Liang YF, Han Y, Wang CF, Jiang C, Xu JR. Targeted deletion of the USTA and UvSLT2 genes efficiently in *Ustilaginoidea virens* with the CRISPR-Cas9 system. Front Plant Sci. 2018;9. https://doi.org/10.3389/fpls.2018.00699 .

Schuster M, Schweizer G, Kahmann R. Comparative analyses of secreted proteins in plant pathogenic smut fungi and related basidiomycetes. Fungal Genet Biol. 2018;112:21–30. https://doi.org/10.1016/j.fgb.2016.12.003.

Schwartz CM, Hussain MS, Blenner M, Wheeldon I. Synthetic RNA polymerase III promoters facilitate high-efficiency CRISPR-Cas9-mediated genome editing in *Yarrowia lipolytica*. Acs Synth Biol. 2016;5:356–9. https://doi.org/10.1021/acssynbio.5b00162.

Song L, Ouedraogo JP, Kolbusz M, Nguyen TTM, Tsang A. Efficient genome editing using tRNA promoter-driven CRISPR/Cas9 gRNA in *Aspergillus niger*. PLoS One. 2018;13. https://doi.org/10.1371/journal.pone.0202868.

Song RJ, Zhai Q, Sun L, Huang EX, Zhang Y, Zhu YL, et al. CRISPR/Cas9 genome editing technology in filamentous fungi: progress and perspective. Appl Microbiol Biotechnol. 2019;103:6919–32. https://doi.org/10.1007/s00253-019-10007-w.

Wang RJ, Cui D, Zhao R, Jin Y, Zeng W, Yang Y, et al. The regulatory subunit MoB56 of PP2A phosphatase regulates pathogenicity, growth and development in a protein complex with the atypical catalytic subunit Ppg1 in the rice blast fungus *Magnaporthe oryzae*. Phytopathol Res. 2023;5:10. https://doi.org/10.1186/s42483-023-00165-1.

Wilson RA, Talbot NJ. Under pressure: investigating the biology of plant infection by *Magnaporthe oryzae*. Nat Rev Microbiol. 2009;7:185–95. https://doi.org/10.1038/nrmicro2032.

Xie KB, Minkenberg B, Yang YN. Boosting CRISPR/Cas9 multiplex editing capability with the endogenous tRNA-processing system. Proc Natl Acad Sci U S A. 2015;112:3570–5. https://doi.org/10.1073/pnas.1420294112.

Yang J, Zhao X, Sun J, Kang Z, Ding S, Xu JR, et al. A novel protein Com1 is required for normal conidium morphology and full virulence in *Magnaporthe oryzae*. Mol Plant Microbe Interact. 2010;23:112–23. https://doi.org/10.1094/MPMI-23-1-0112.

Zhang YP, Wang J, Wang ZB, Zhang YM, Shi SB, Nielsen J, et al. A gRNA-tRNA array for CRISPR-Cas9 based rapid multiplexed genome editing in *Saccharomyces cerevisiae*. Nat Commun. 2019;10. https://doi.org/10.1038/s41467-019-09005-3.

Zheng XM, Zheng P, Zhang K, Cairns TC, Meyer V, Sun JB, et al. 5S rRNA promoter for guide RNA expression enabled highly efficient CRISPR/Cas9 genome editing in *Aspergillus niger*. Acs Synth Biol. 2019;8:1568–74. https://doi.org/10.1021/acssynbio.7b00456.